Langmuir, Available online 3 March 2026
DOI: 10.1021/acs.langmuir.5c06371

Complex formation mechanism between β-cyclodextrin and organic micropollutants in water, studied by molecular dynamics simulations

Oscar De Vince[1], Zhewen Duan[2], Zhugen Yang[2], Yann Chevolot[3], Christelle Yeromonahos[1*]

[1]Ecole Centrale de Lyon, INSA Lyon, CNRS, Universite Claude Bernard Lyon 1, CPE Lyon, INL, UMR5270, 69130 Ecully, France

[2]Cranfield University, Faculty of Engineering and Applied Sciences, Cranfield MK43 0AL, United Kingdom

[3]CNRS, Ecole Centrale de Lyon, INSA Lyon, Universite Claude Bernard Lyon 1, CPE Lyon, INL, UMR5270, 69130 Ecully, France

*Corresponding author: christelle.yeromonahos@ec-lyon.fr

Abstract

Cyclodextrin are cage molecules with a hydrophilic exterior that promotes their solubility in water while their hydrophobic cavity allows the encapsulation of low molecular weight organic molecules. Thus, cyclodextrin are promising compounds for removing micropollutant molecules from water. The binding mechanism of ligand molecules to the cavity of the cyclodextrin is driven by the physico-chemical properties of the ligand such as its hydrophilic/hydrophobic balance and by its number of hydrogen bond donors and acceptors. In the present study, the free binding energy of nine different organic micropollutant molecules (bisphenol A, the charged and the uncharged forms of trimethoprim, the predominant forms of tetracycline at pH1, pH4 and pH8, caffeine, theobromine, and atenolol) to β-cyclodextrin are calculated by molecular dynamics simulations using steered-molecular dynamics and umbrella sampling analysis. Steered molecular dynamics and umbrella sampling analysis are shown to yield similar values for the free binding energy of the complexes, closed to the experimental values. Then, the contributions of the electrostatics and van der Waals interactions to the free binding energy of the complexes are investigated, highlighting the major impact of van der Waals interactions. Finally, the effect of the number of hydrogen bonds between β-cyclodextrin and ligand molecules on their free binding energy is shown to depend on the octanol/water partition coefficients, logD, of the ligands. In particular, a correlation between the number of hydrogen bonds and the free binding energy of the complexes is demonstrated in the case of ligand molecules with logD values comprised in the range -0.55 – 0.92.

Published by ACS. This is the Author Accepted Manuscript issued with: Creative Commons Attribution License (CC:BY 4.0).
The final published version (version of record) is available online at DOI:10.1021/acs.langmuir.5c06371. Please refer to any applicable publisher terms of use.

Abbreviations

CD **Cyclodextrin**

β-CD **β-Cyclodextrin**

MD **Molecular Dynamics**

SMD **Steered Molecular Dynamics**

NVT **Number of particles Volume Temparature**

NPT **Number of particles Pressure Temperature**

SASA **Solvent Accessible Surface Area**

CSA **Contact Surface Area**

RMSD **Root Mean Square Deviation**

MW **Molar Weight**

Rg **Radius of gyration**

H-bonds **hydrogen bonds**

BPA **Bisphenol A**

Tetra. **Tetracycline**

Theo. **Theobromine**

Trim. **Trimethoprim**

ΔG_{SMD} **Free binding energy determined by Steered Molecular Dynamics simulations**

$\Delta G_{Umbrella}$ **Free binding energy determined by Umbrella sampling**

ΔG_{exp} **experimental Free binding energy**

ΔG_{sr} **Electrostatic and van der Waals contributions to the enthalpy part of the free binding energy**

Introduction

Cyclodextrins (CD) are an attractive host in the field of host-guest chemistry due to their hydrophobic cavity that can encapsulate organic ligands while their hydrophilic exterior promotes water solubility. Consequently, cyclodextrins are widely used as solubiliser of hydrophobic compounds particularly in pharmaceutical industry and are promising compounds for removing micropollutants from water by means of adsorption.[1,2]

The hydrophobicity of the ligands as well as their ability to form hydrogen bonds within the CD cavity are major factors that govern the binding between cyclodextrin and ligands.[3] Škvára *et al.* demonstrated that the average number of intermolecular hydrogen bonds between ibuprofen and β -cyclodextrin is equal to 0.4 for the most stable configurations of the complex while it decreases by 33% for the less stable conformations of the complex.[4] In addition, González-Méndez *et al.* studied adamantane-doxorubicin prodrugs and found the drugs would undergo conformational changes on binding to decrease the size of the drug molecule so that the most hydrophobic regions are able to fully fit inside the cyclodextrin cavity.[5] Also, when investigating the binding of ketoprofen to a range of cyclodextrins (α, β, substituted β, and γ), Zhao *et al.* found that the involvement of hydrogen bonding vs hydrophobic effect decreases when the ring size increases.[6] Furthermore, some studies have reported that van der Waals forces may be a crucial parameter in governing the binding between CD and ligands molecules.[7] Additionally, machine learning techniques were used to model the impact of 39 physico-chemical parameters of 3000 different ligand molecules on their binding energy with several types of CD.[8] The model suggests that the main factors that impact CD-ligand binding are the size, solvent accessible surface area, water-octanol partition coefficient, and polarizability of the ligands. However, other models have found different parameters, such as LUMO energy to be significant. [9–11] Nevertheless, to the best of our knowledge, the main factors that impact the binding energy of CD-ligand complexes for given hydrophilic/hydrophobic properties of the ligands have never been investigated.

The binding energy of CD-ligand complexes can be determined by different experimental techniques such as spectrophotometry[12,13], chromatography[14], differential scanning calorimetry[15], mass spectrometry[16], and thermogravimetry[17]. The binding energy is in the range of 0 to −40 kJ mol^{-1} for most of the complexes (or in the range of 0 to -30 kJ mol^{-1} for only β-cyclodextrin). There is also a great range of classical computational methods for determining binding energy. Docking was used by da Silva *et al.* leading to a docking binding energy of -14.6 kJ mol^{-1} for the studied β-cyclodextrin complex while the experimental energy was -22.3 kJ mol^{-1}.[18,19] A few studies have shown that steered molecular dynamics yield binding energy with a better accuracy than docking.[19–22] For example, Caballero *et al.*

calculated a binding energy of -96 kJ mol^{-1} for the progesterone-β-cyclodextrin complexes close to the experimental value (-120 kJ mol^{-}1).[23] Nevertheless, this complex is far more stable than most of the cyclodextrin complexes. Umbrella sampling method was also used to determine binding energy of β-cyclodextrin complex.[21,24,25] A binding energy of -30.5 kJ mol^{-1} was found, close to the experimental value of -24.0 kJ mol^{-1}.[26] Additionally, they find that hydrogen bonding is strongly correlated with the binding energy profile suggesting that hydrogen bonds are a key factor in the complex stabilization. Finally, several studies have demonstrated that MMPBSA analysis combined to molecular dynamics simulations allow to investigate qualitatively the binding energy of cyclodextrin complexes. [18,26,27] In particular, Suárez *et al.* produced a model which relates the results of the computational MMPBSA binding energy method of 57 ligands to experimental binding energy.[27] They find that while the raw MMPBSA energy values do not match experimental observations, the computational results are nonetheless linearly correlated with the experimental energy. In addition to these methods, quantum mechanical and empirical techniques have also been developed.[27] The computing cost and the deviation from the experimental value vary between the methods. Nevertheless, to the best of our knowledge, the accuracy of the different simulation methods for calculating the binding energy of a given CD-ligand complex has never been studied.

In this work, the accuracy of steered molecular dynamics and umbrella sampling analysis on the calculated binding energy of nine different β-cyclodextrin (β-CD) complexes is studied. The calculated values are compared to experimental values previously published. Then, effects of van der Waals, electrostatic and polar interactions, and hydrogen bonds between β-CD and the nine ligands molecules, on the free binding energy of the complexes, are shown to vary depending on the hydrophilic/hydrophobic properties of the ligands. The nine ligand molecules include: bisphenol A (BPA), the charged and the uncharged forms of trimethoprim (named charged Trim. and uncharged Trim. hereafter), the predominant forms of tetracycline at pH1, pH4 and pH8 (named Tetra. pH1, Tetra. pH4 and Tetra. pH8 hereafter), caffeine, theobromine (named Theo. hereafter) and atenolol. The protonated states of these ligand molecules are presented in Table S1. These molecules are known to be aquatic pollutants. BPA is an industrial chemical molecule used in the production of polycarbonate plastics.[28] Trimethoprim and tetracycline are both antibiotics.[29] Caffeine is the most widely consumed drug globally.[30] Theobromine is a biologically active metabolite of caffeine. Atenolol is a widely prescribed β-blocker.[31] While these nine ligand molecules have similar molecular weights (180-440 g mol^{-1}), they have different hydrophobic/hydrophilic properties (with an octanol/water partition coefficient, logD, varying from -6.82 for Tetra. pH8, the most hydrophilic ligand studied, to 4.04 for BPA, the most hydrophobic ligand studied), different proportions of aromatic cycles, and different

numbers of hydrogen bond donors and acceptors (varying from 2 donors and 2 acceptors for BPA to 6 donors and 9 acceptors for Tetra. pH7).[32]

Materials and Methods

Docking simulations

The three-dimensional conformations of the nine ligand molecules were generated using OpenBabel gen3d version 3.3.1, using the OPLS-AA force field in the chemical identifier SMILES. The three-dimensional structure of β-CD (COD-CID 444041) from PubChem was used and converted into the pdb format through OpenBabel. Docking simulations employed the Autodock vina version 1.1.2. The simulation boxes were defined around the coordinates of β-CD, and were sufficiently large to contain both β-CD and the ligand molecule studied. Thus, the box size was 15.0 x 22.5 x 18.0 Å, with a grid spacing of 0.375 Å. Molecular docking simulations were performed by using an exhaustiveness parameter equal to 30, 10 kcal/mol in energy range, 20 modes, and a seed parameter equal to -150.[18] pKa were calculated using Chemaxon software in order to determine the protonation status of the ligand for the studied pH. The molecule structures were drawn and modeled accordingly.

MD simulations and analysis parameters

The most stable conformations from docking were used as the initial structures for MD simulations. LigParGen was used to generate topology files for β-CD and ligand molecules. The MD simulations were performed with the Gromacs simulation package, version 2023.3 and visualization was done using the VMD software package version 1.9. The OPLS all-atom force-field was used. Water model TIP3P was described with OPLS all-atom force field.[33,34] Where necessary the electrical charges of ligands were neutralised using Na^+ or Cl^- ions. Firstly, energy minimization was performed with the Steepest Descent method, followed by NVT and NPT equilibrations of 100 ps each. Then, production runs were carried out for 250 ns, with 3 independent runs for all the complexes studied. The integration of the equations of motion was done using a leap-frog algorithm and a time step of 2 fs. A LINCS algorithm was used to apply constraint to bond parameters. Temperature was maintained at 300 K with a Nose-Hoover thermostat and a time constant of 0.4 ps. The pressure was kept at 1 bar using a Parrinello-Rahman barostat, with a time constant of 2 ps. Long-range electrostatic interactions were calculated with the particle-mesh Ewald method and a cutoff of 1 nm. The same cutoff was used for LJ potentials.

The minimum distance between β-CD and ligand molecules was calculated from the 250ns MD simulations using *gmx mindist* during the entire 250ns simulation. A molecule is defined as bound when the minimum distance is below 0.5 nm. The percentage adsorption was calculated as the percentage of time when the molecule is bound. Standard deviations were calculated from the triplicate MD runs.

The root means square deviation (RMSD), radius of gyration (Rg), SASA, and H-bond number between β-CD and a ligand molecule were calculated from the 250ns MD simulations using gmx RMSD, gyrate, sasa, and hbond respectively, by averaging the values obtained during all the bound states of the complexes. Indeed, because of the succession of bound and unbound states, no permanent equilibrium state is reached. RMSD refers to the global conformation change of molecules. RMSD values were calculated separately for the ligand molecules and for the β-CD molecule in the bound states, with respect to their structures alone in water. Standard deviations were calculated from the triplicate MD runs.

The contact surface area (CSA) measures the area which is in contact between β-CD and a ligand molecule. It is calculated using the following equation:

$$CSA = - 0.5 (SASA_{comp} - [SASA_{lig} + SASA_{cd}]) \qquad (1)$$

where SASA is the solvent accessible surface area calculated using the van der Waals radius of the molecules involved. $SASA_{lig}$ and $SASA_{cd}$ refer to the free ligand and free β-cyclodextrin in water. A larger CSA shows a greater contact area between β-CD and the ligand molecule. SASA values were calculated as averages over the bound states of each complex during the 250ns MD simulations. Standard deviations were calculated from the triplicate simulations.

Energy calculation

SMD simulations. The more stable conformations from docking simulations, followed by an MD energy minimization, NVT and NPT equilibrations of 100 ps each (as described above), were used as the starting configurations for SMD simulations. Non-equilibrium SMD simulations were performed, by applying an external force to the ligand molecule to unbind it from β-CD. The center of mass of β-CD was fixed. Force was applied to the ligand molecule by a harmonic potential with a spring constant k = 1000 $kJ.mol^{-1}.nm^{-2}$ and a velocity *v* = 0.2 m/s.[35,36] The ligand molecule was pulled away from β-CD in the Z-direction where the vector between the center of masses of β-CD and the ligand lies and facing

such that the ligand would be pulled through the larger ring in the cavity. The Z-direction was defined as perpendicular to the plane formed by the oxygen atoms belonging to the largest ring of β-CD. The ligand is pulled from β-CD through the largest ring to the conical barrel as the smallest ring would present considerable steric hindrance. This is supported by the fact that no ligands dissociated through the smaller ring during MD simulations. Ten replicates of 10 ns SMD simulations were run for each complex.

Jarzynski's equality was used to derive the free binding energy difference from the external work, obtained by integration of the steering force along the pathway from SMD trajectories. Work v. Time curves were converted into ΔG_{SMD} v. displacement by placing the time-based data in bins of 0.01 nm (ΔG_{SMD} value did not change at bin widths smaller than 0.01nm). The free binding energy was deduced from the exponential average calculation. The standard deviation of ΔG_{SMD} was calculated by using bootstrapping, with 10 iterations.

umbrella sampling. This method has been widely used for improving conformational sampling and free energy calculations.[37,38] A random SMD trajectory was chosen to act as a reference frame. A python script was used to find the frames closest to certain distance intervals between β-CD and ligand molecules. Intervals of 0.1 nm were chosen for intermolecular distances less than 1 nm and 0.2 until 2.6 nm. Next for each interval NPT equilibration was performed (100 ps, Berendsen thermostat). A production run was executed (10 ns, Nosé-Hoover thermostat, Parrinello-Rahman barostat, Langevin integrator) with a fixed potential of 1000 kJ mol^{-1} nm^{-2} in the Z-axis. Using the distribution of distance from the centre of the potential against time and the initial simulation parameters, gmx WHAM was used to generate the potential of mean force curve, from which the binding energy $\Delta G_{umbrella}$ was extracted. Umbrella sampling variables were chosen such that there was a stronger restraining potential when the ligand was close to the cyclodextrin and a weaker potential further from the cyclodextrin. The standard deviation of $\Delta G_{umbrella}$ was calculated by using bootstrapping, with 50 iterations.

Interaction energy between β-CD and ligand molecules ΔG_{sr} was calculated by adding the electrostatic and Van der Waals interaction energies obtained using the function from Gromacs gmx energy.[39] The standard deviation of ΔG_{sr} was calculated from three replicate MD simulations.

Results and Discussion

The binding of β-CD to the nine different ligand molecules was studied through 250ns MD simulations. All the ligand molecules were found to be trapped inside the cavity of β-CD, except Tetra. pH8 that is

adsorbed at the top outer surface of the cavity. **Figure 1** shows the complexes formed between β-CD and BPA, and between β-CD and Tetra. pH8. All the other studied complexes are presented in **Figure S1**. The number of binding and unbinding events during the 250ns MD simulations varies between the complexes studied. The time percentages during which each ligand molecule is bound to β-CD (%adsorp.) are given in **Table 1.** BPA and uncharged Trim. molecules stay bound to β-CD during the entire 250ns MD simulations, while Tetra. pH8 is bound to β-CD only during half of the 250ns MD simulations. The six other ligand molecules are bound to β-CD between 95% and 67% of the 250ns MD simulation. In spite of high error bars in the case of the smallest adsorption percentages, these results are in line with the free binding energies of the complexes discussed below.

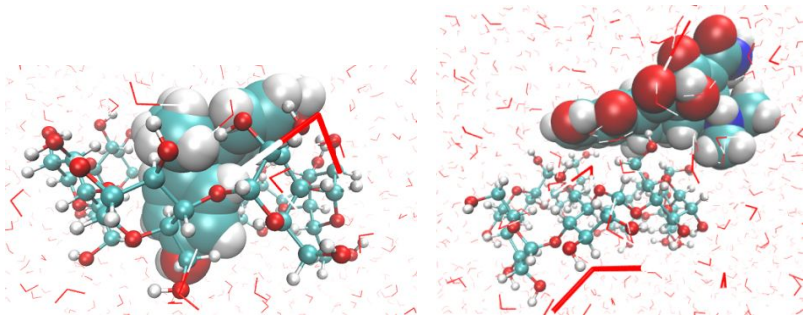


Figure 1. (left) BPA and (right) Tetra. pH8 bound to the β-CD cavity.

Calculation of the free binding energy between β-CD and ligand molecules

The free binding energies between β-CD and ligand molecules were calculated by SMD simulations (ΔG_{SMD}). For each complex, at least ten SMD replicates were run for 10 ns at 0.2 m/s. The Jarzinski modeling from the force-time curves is given in **Figure S2** for all the complexes studied. The ΔG_{SMD} values are indicated in **Table 1**, along with the experimental free binding energies values obtained through previous studies (ΔG_{exp}).[40-45] A correlation is obtained between ΔG_{SMD} and ΔG_{exp}, as shown in **Figure 2**. Note that at pH7, about half of the trimethoprim molecules are uncharged while the other half are positively charged, while ΔG_{exp} is given at pH 7 independently of the charge state of trimethoprim. The best correlation between ΔG_{SMD} and ΔG_{exp}, are obtained in the case of the three ligand molecules with the lower ΔG_{exp}, therefore the most negative free binding energies. Indeed, the differences between ΔG_{SMD} and ΔG_{exp} are only 2%, 2% and 27% respectively for BPA, theobromine, and Tetra. pH4. The differences between ΔG_{SMD} and ΔG_{exp}, for the trimethoprim, atenolol, and caffeine are in the range 47% - 74%.

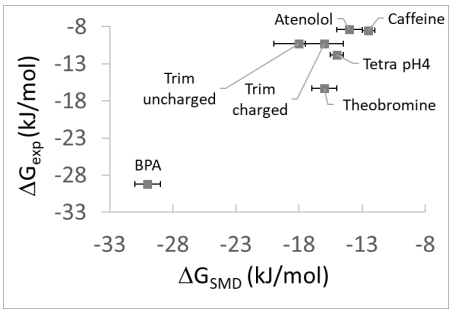
Table 1. Time percentages of the 250ns MD simulations during which each ligand molecule is bound to β-CD (**%adsorp.**). Free binding energy between β-CD and ligand molecules calculated by SMD simulations (ΔG_{SMD}) and

umbrella sampling ($\Delta G_{Umbrella}$). Sum of the electrostatic and VdW interaction energies between β-CD and ligand molecules (ΔG_{sr}). Free binding energy between β-CD and ligand molecules obtained from previous experimental studies (ΔG_{exp})[40-45]. All the values of energy are given in kJ/mol. Standard deviations are indicated.

	BPA	uncharged Trim.	Tetra. pH1	Theo.	charged Trim.	Tetra. pH4	Atenolol	Caffeine	Tetra. pH8
%adsorp.	0.99± 0.01	1.00± 0.00	0.93± 0.06	0.95± 0.03	0.95± 0.07	0.91± 0.11	0.67± 0.20	0.80± 0.06	0.50± 0.20
ΔG_{SMD}	-30± 2	-18± 4	-17± 2	-16± 2	-16± 3	-15± 1	-14± 2	-12± 1	-4± 2
$\Delta G_{Umbrella}$	-27± 2	-20± 2	-17± 1	-14± 1	-5± 1	-14± 3	-11± 2	-12± 1	-8± 4
ΔG_{sr}	-117± 18	-156± 34	- 107± 54	-110± 41	-96± 34	-132± 56	-66± 55	-60± 40	-44± 49
ΔG_{exp}	-29.2	-10.3	-	-16.3	-10.3	-11.8	-8.4	-8.5	-

In addition, the free binding energies of the studied complexes were calculated by umbrella sampling. The bias distributions and the potential of mean forces are shown in **Figure S3 and Figure S4**, while the $\Delta G_{umbrella}$ are reported in **Table 1**. ΔG_{SMD} and $\Delta G_{umbrella}$ are shown to be in excellent agreement, except for the charged Trim. Indeed, the free binding energy of charged Trim. calculated by SMD is -16 kJ/mol, and -5 kJ/mol when calculated by umbrella sampling. This difference was observed on three independent replicates and stays unexplained. Nevertheless, for charged Trim., the difference between ΔG_{SMD} and ΔG_{exp} (55%) is similar to the one obtained between $\Delta G_{umbrella}$ and ΔG_{exp} (51%). Thus, SMD and umbrella sampling analysis were demonstrated to allow for predicting the free energy binding of the studied complexes, with a similar precision, that increases as the free binding energy decreases. The Pearson correlation coefficient between ΔG_{SMD} and ΔG_{exp} is equal to 0.82, while this coefficient is equal to 0.73 between ΔGumbrella and ΔGexp.

Finally, the sum of the electrostatic and Lennard Jones interactions, indicated in **Table 1 (ΔG_{sr})**, is poorly correlated to ΔG_{exp}.



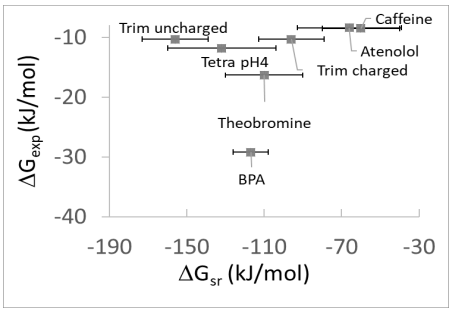


Figure 2. The free binding energies between β-CD and ligand molecules calculated by SMD simulations (ΔG_{SMD}), and the sum of the electrostatic and van der Waals energies between β-CD and ligand molecules (ΔG_{sr}) v. the experimental free binding energies values obtained through previous studied (ΔG_{exp})[40-45].

The electrostatic (ΔG_{elec}) and van der Waals (ΔG_{VdW}) contributions to ΔG_{sr} are presented in **Table 2**. The values of ΔG_{VdW} roughly decrease (become more favorable) as the free binding energies (ΔG_{SMD}) of the complexes decrease, while the values of ΔG_{elec} are not correlated to the free binding energy of the molecules studied (**Figure 3**). The Pearson correlation coefficient between ΔG_{vdw} and ΔG_{SMD} is equal to 0.76. Thus, these results demonstrate that VdW interactions are a major parameter that controls the free binding energy between β-CD and the ligand molecules studied.

Table 2. Electrostatic and van der Waals contributions to the enthalpy part of the free binding energy between β-CD and the ligand molecule studied.

	BPA	uncharged Trim.	Tetra. pH1	Theo.	charged Trim.	Tetra. pH4	Atenolol	Caffeine	Tetra. pH8
ΔG_{elec}	-22± 2	-70± 2	-70± 2	-52± 2	-26± 2	-63± 2	-50± 2	-16± 1	-24± 2
ΔG_{VdW}	-83± 1	-83± 1	-86± 1	-68± 1	-83± 1	-76± 1	-54± 1	-63± 1	-28± 1

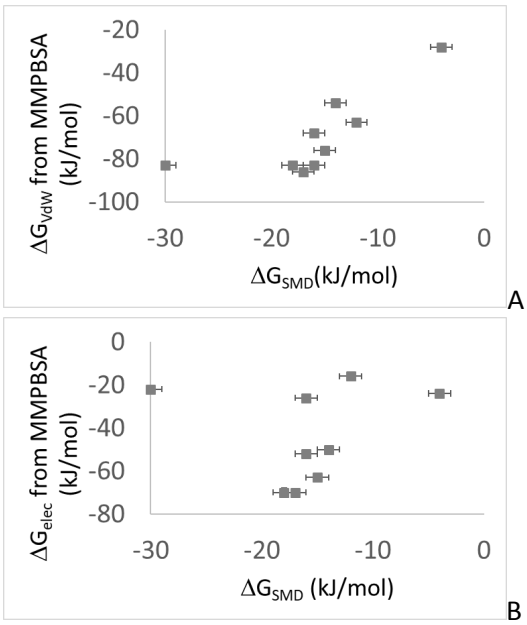


Figure 3. (A) The van der Waals (ΔG_{vdW}) and (B) the electrostatic (ΔG_{elec}) contributions to the enthalpy part of the free binding energy between β-CD and ligand molecules v. the free binding energy calculated by SMD analysis (ΔG_{SMD}).

Impact of the hydrophilic-hydrophobic properties of the ligand molecules studied on the free binding energy of the complexes

The physico-chemical parameters of the studied ligands molecules (molar mass, log D, and the proportion of aromatic cycles) are presented in **Table 3**. Aromatic proportions are calculated as the fraction of aromatic atoms compared to all atoms in a given ligand. The molar masses of the nine ligand molecules are close, spanning in the range 194 g/mol (caffeine) – 445 g/mol (Tetra. pH1), and are not correlated to the free binding energy of the complexes, as shown in **Figure 4**. Nevertheless, the log D values of the ligands studied are variable. Indeed, BPA is the most hydrophobic ligand (log D = 4.04), while Tetra. pH8 is the most hydrophilic ligand (log D = -6.82), and the seven others ligand have intermediate log D values comprised between -4.67 and 0.92. In line with the log D values, BPA has the highest proportion of aromatic cycles (0.71), while Tetra. has the lowest proportion of aromatic cycles (0.18), with the seven other molecules studied lying between 0.32 and 0.57 aromatic cycles. LogD values, as well as the proportion of aromatic cycles, roughly increase as ΔG_{SMD} becomes more favorable, as shown in **Figure 4**. The Pearson correlation coefficient between logD and ΔG_{SMD} is equal to 0.79 while this coefficient is equal to 0.72 between thee aromatic proportion and ΔG_{SMD}. Indeed, BPA has the lowest ΔG_{SMD} (-30 kJ/mol), while Tetra. pH8 has the highest ΔG_{SMD} (-4 kJ/mol), and the seven other studied molecules have intermediate ΔG_{SMD} (from -18kJ/mol to -12kJ/mol). This result is

expected as the cavity of β-CD is hydrophobic. In addition, this result is in line with a previous study that has demonstrated that the presence of an aromatic ring in alcohol dehydrogenase is responsible for the formation of the complex with CD.[46] Thus, logD seems to be a major parameter that controls the free binding energy between β-CD and highly hydrophobic (logD around 4) or highly hydrophilic (log D around -6) ligand molecules. Nevertheless, variations of logD between -4.67 and 0.92 are not sufficient to explain the variations in the free binding energy of the complexes.

In addition, the free binding energy of the complexes studied (ΔG_{SMD}) is shown to be correlated to the number of water molecules in the cavity of β-CD during bound states (Pearson correlation coefficient is equal to 0.89) (**Figure 4**). Indeed, 3.86 water molecules are present in the cavity of β-CD alone in water (without any ligands molecules), while this value drops to 0.14 when BPA (the ligand molecule with the most favorable free binding energy) is bound, and to 3.64 when Tetra. pH8 (the ligand molecule with the most unfavorable free binding energy) is bound (Table 3). The high number of water molecules in the cavity, in the case of Tetra. pH8, reflects the shallow trapping of the molecule. Thus, the binding mechanism between β-CD and the ligand molecules studied involves expulsion of water molecules from the β-CD cavity.

Table 3. Molar mass (MW), logD, and proportion of aromatic cycles of the different ligand molecules studied. Mean number of water molecules in the β-CD cavity when the different ligand molecules are bound to β-CD. The number of water molecules in the β-CD cavity, without any ligands, is equal to 3.9± 1.9. Mean number of hydrogen bonds (H-bonds) between β-CD and the ligand molecules. Mean value of the contact surface area (CSA) between β-CD and the ligand molecules. Mean RMSD values of ligands and of β-CD. Each average is calculated from the bonding states only of the 250ns MD simulations. Standard deviations are calculated from triplicate MD runs.

	BPA	uncharged Trim.	Tetra. pH1	Theo.	charged Trim.	Tetra. pH4	Atenolol	Caffeine	Tetra. pH8
MW (g/mol)	228	290	445	180	291	444	266	194	443
logD	4.04	0.92	-4.67	-0.41	0.92	-3.83	-1.8	-0.55	-6.82
aromatic proportion	0.71	0.57	0.18	0.38	0.57	0.18	0.32	0.36	0.18
# water molecules in the β-CD cavity	0.14± 0.4	0.63± 0.7	2.31± 2.1	1.31± 1.0	1.51± 1.0	1.71± 1.7	1.89± 1.5	2.03± 1.7	3.64± 1.8

# H-bonds	0.38± 0.01	1.73± 0.07	1.03± 0.32	0.95± 0.30	1.05± 0.54	0.82± 0.65	0.35± 0.15	0.15± 0.01	0.21± 0.31
CSA (nm²)	2.46± 0.20	2.67± 0.16	1.46± 0.53	1.76± 0.29	1.9± 0.28	1.52± 0.35	1.01± 0.60	1.25± 0.44	0.60± 0.51
rmsd ligand (nm)	0.114± 0.005	0.151± 0.011	0.094± 0.020	0.029 ± 0.001	0.169± 0.004	0.127± 0.010	0.222± 0.001	0.033± 0.000	0.241± 0.002
rmsd β-CD (nm)	0.110± 0.013	0.105± 0.007	0.131± 0.014	0.125 ± 0.020	0.112± 0.018	0.151± 0.026	0.154± 0.021	0.165± 0.021	0.151± 0.011

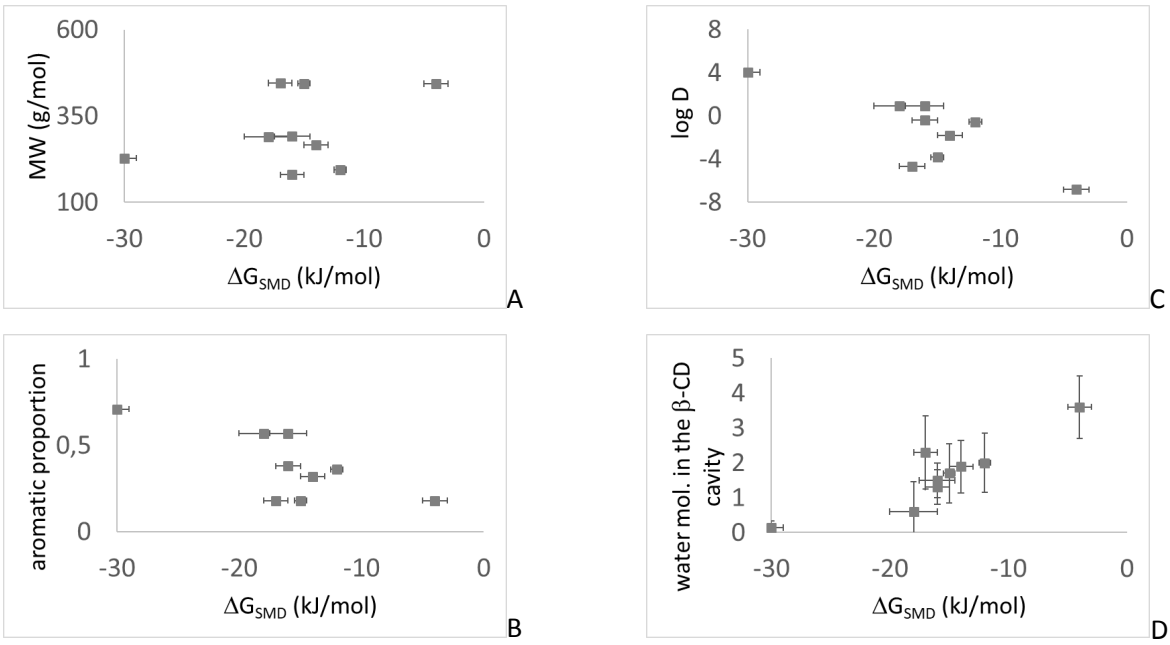


Figure 4. (A) Molar mass (MW), (B) proportion of aromatic cycles, and (C) logD of the different ligand molecules studied v. ΔG_{SMD}. (D) Mean number of water molecules in the β-CD cavity when the different ligand molecules are bound to β-CD v. ΔG_{SMD}. Each average is calculated from the bound states only, of the 250ns MD simulations. Standard deviations are calculated from triplicate MD runs.

Impacts of H-bonds on the free binding energy between β-CD and the ligand molecules studied

The average number of H-bonds between β-CD and the ligand molecules studied, during the bound states of the complexes, are indicated in **Table 3**. Both BPA and Tetra. pH8 have low h-bond numbers (0.38 and 0.21 respectively). Thus, H-bonds do not impact significantly the free binding energy of the most hydrophilic and hydrophobic molecules studied. Indeed, ΔG_{SMD} is -30kJ/mol for BPA and -4kJ/mol for Tetra. pH8. However, for the seven other molecules with intermediate logD, the number of H-bonds increases as ΔG_{SMD} decreases (become more favorable) (**Figure 5**). Thus, these results demonstrate that the number of H-bonds between β-CD and the ligand molecules studied with intermediate logD, is a major parameter, along with VdW interactions, that controls the free binding energy of the complexes. This result may seem counterintuitive since hydrogen bonds increase the polarity of a complex and therefore would be expected to decrease the binding. However, β-CD does contain seven ether groups within the cavity, that are hydrogen bond acceptors. Finally, the large standard deviations for the number of hydrogen bonds reflect the variety of conformations whether the complex is strongly (e.g. theobromine) or weakly (e.g. Tetra. pH8) bound. Note that the part of the binding energy associated to H-bonds is included in the ΔG_{elec} values, even if ΔG_{elec} is not correlated to the binding energy of the complexes.

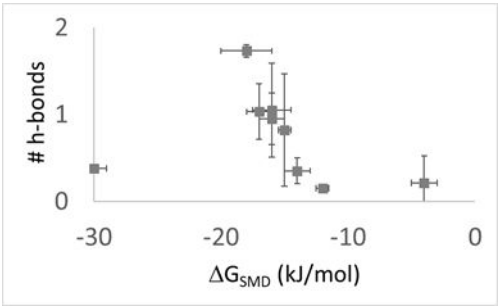


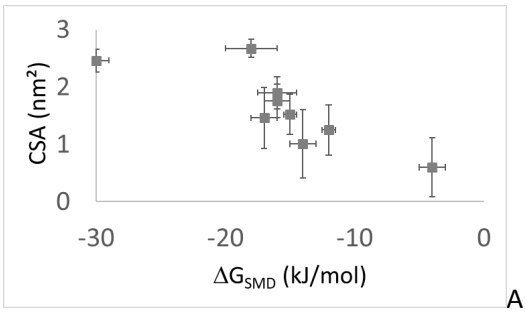
Figure 5. Mean number of hydrogen bonds (H-bonds) between β-CD and the ligand molecules v. ΔG_{SMD}. Averages are calculated from the bonding states only of the 250ns MD simulations. Standard deviations are calculated from triplicate MD runs.

Structure of the β-CD – ligand molecule complex.

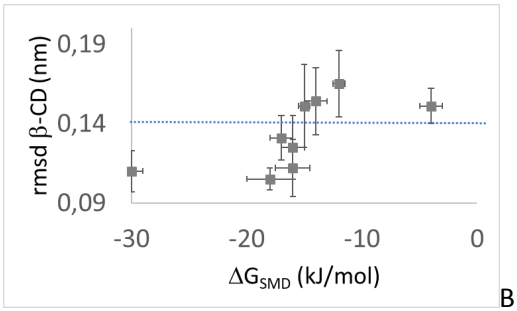
The mean contact surface (CSA) area between the β-CD and the different ligand molecules during bound states, as well as the mean rmsd values of the ligand molecules and of β-CD during bound states are given in **Table 3**, and their variations with ΔG_{SMD} are presented in **Figure 6**. The CSA is shown to increase as ΔG_{SMD} decreases (become more favorable). This result agrees with the increase in van der

Waals interactions, as ΔG_{SMD} decreases, discussed above. Moreover, the CSA increase involves an increase in the rigidity of β-CD. Indeed, the rmsd values of β-CD decrease as ΔG_{SMD} decreases, as shown in **Figure 6**, becoming lower than the rmsd of β-CD alone in water. In addition, the rmsd of the β-CD-ligand complexes resembles a bimodal distribution centered around 0.1 and 0.2 nm which corresponds to a circle and oval shaped ring respectively, as shown in **Figure 7**. In the case of the ligand molecules with the more favorable ΔG_{SMD}, the predominant form is the circular, while in the case of the ligand molecules with the less favorable ΔG_{SMD}, the distribution is balanced between oval and circle forms. Such a balance between oval and circle forms is also obtained for β-CD alone in water.

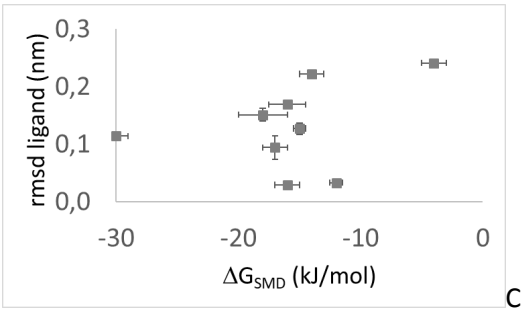
Nevertheless, the rmsd of the ligand molecules alone seems to be independent on the free binding energy (**Figure 6)**. In addition, the RMSD of all the ligand molecules studied stay constant (equal to the values given in **Table 3**) independently of their bound and unbound states.



A

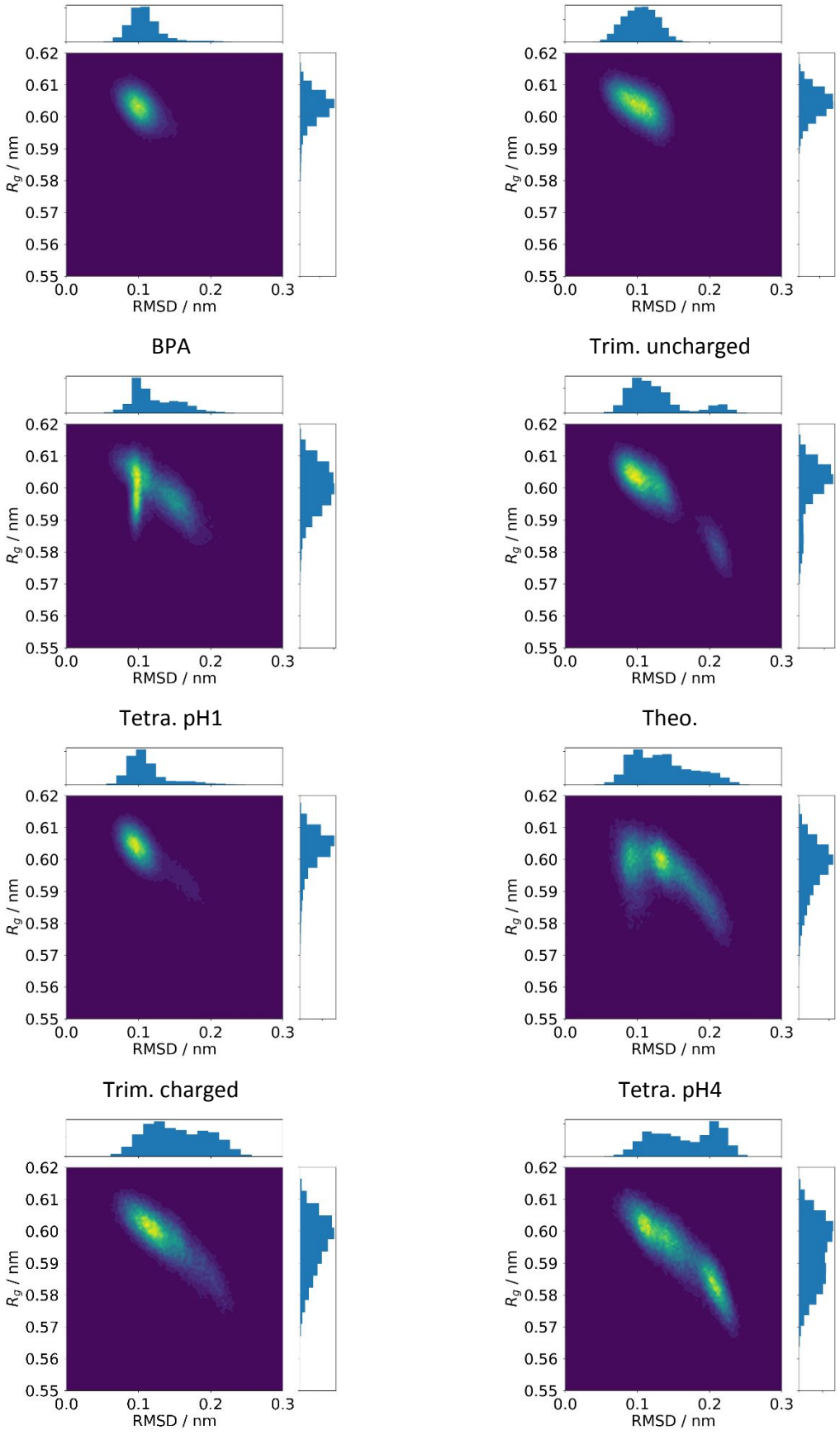


B



C

Figure 6. (A) Mean value of the contact surface area (CSA) between β-CD and the ligand molecules v. ΔG_{SMD}. Mean RMSD values of β-CD (B) and of ligands (C) v. ΔG_{SMD}. The blue dot line on Figure 6.B indicates the rmsd value of β-CD alone in water. Averages are calculated from the bonding states only of the 250ns MD simulations. Standard deviations are calculated from triplicate MD runs.


BPA
Trim. uncharged
Tetra. pH1
Theo.
Trim. charged
Tetra. pH4
R_g / nm
RMSD / nm
0.55
0.56
0.57
0.58
0.59
0.60
0.61
0.62
0.0
0.1
0.2
0.3

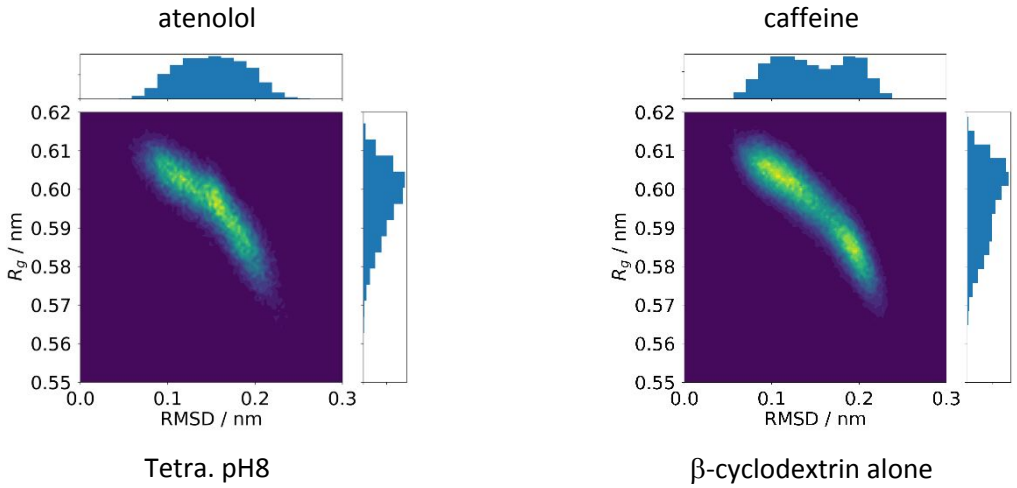


Figure 7. Relative frequency of rmsd (nm) and Rg (nm) for the different complex studied, during bound states, as well as for β-CD alone in water, over the 250ns MD simulation.

Conclusions

The binding of β-CD to nine different ligand molecules was studied by MD simulations, during 250ns. Each complex was undergoing various numbers of unbinding and binding events over the 250ns. Indeed, BPA and uncharged Trim. molecules stayed bound to β-CD during the entire simulation, while the cumulation of unbinding events of Tetra. pH8 to β-CD showed that the cumulative adsorption time was 50% of the 250 ns. The six other ligand molecules yielded intermediate percentage of adsorption, in the range of 95% - 67%. These adsorption percentages are in line with the free binding energy of the complexes calculated through SMD simulations, ΔG_{SMD}. Moreover, the values of ΔG_{SMD} agree with the experimental values of the free binding energy from previous studies. The differences between ΔG_{SMD} and ΔG_{exp} are only 2%, 2% and 27% for BPA, theobromine, and Tetra. pH4 respectively, which are the three ligand molecules studied with the most favorable ΔG_{exp}. The differences between ΔG_{SMD} and ΔG_{exp}, for trimethoprim, atenolol, and caffeine are in the range of 47% - 74%. In addition, the free binding energies of the different complexes were calculated using umbrella sampling simulations. The differences between $\Delta G_{umbrella}$ and ΔG_{exp} were similar to the ones between ΔG_{SMD} and ΔG_{exp}, for all the systems. Thus, SMD simulations require less calculation time and therefore seem well adapted to the evaluation of the free energy between β-CD and the ligand molecules studied. Also, the van der Waals contribution to the enthalpy is demonstrated to be qualitatively correlated to ΔG_{SMD}, while the electrostatic part of the enthalpy is not correlated to ΔG_{SMD}. Finally, ΔG_{SMD} is shown to increase as the contact surface area between β-CD and the ligand molecules increases.

In addition, the number of H-bonds between β-CD and the most hydrophobic (BPA) and the most hydrophilic (Tetra. pH8) ligand molecules were found to have a minor impact on their free binding

energy, which are respectively the more and the less favorable energies among the nine complexes studied. Nevertheless, the number of H-bonds between β-CD and ligand molecules with intermediate logD has a major effect on their free binding energies. Finally, in the case of the studied complexes with the more favorable free binding energy (the lowest negative values), β-CD is constrained to a circular shape, while in the case of complexes with the less favorable free binding energy (as well as in the case of β-CD free in water), β-CD is more flexible with a shape that can switch between circular and oval forms.

The research findings could support to predict interactions between cyclodextrin and ligand molecules and to optimize the functionalization of cyclodextrin for ligand molecules adsorption.

SUPPORTING INFORMATION

Table S1. The protonated states of the nine ligand molecules studied. **Figure S1.** The complexes formed between β-CD and the nine ligands studied, in water. **Figure S2.** The Jarzinski modeling from the force-time curves for all the complexes studied. **Figure S3.** The bias distributions from umbrella sampling for all the complexes studied. **Figure S4.** The potential of mean forces from umbrella sampling for all the complexes studied.

AUTHOR INFORMATION

Author Contributions

The manuscript was written through contributions of all authors. All authors have given approval to the final version of the manuscript.

FUNDING SOURCES

This work was supported by the Ecole Supérieure de Physique Chimie Electronique de Lyon (CPE) for founding the internship of Oscar De Vince. Z.D. and Z.Y. were supported by The Leverhulme Trust Research Leadership Awards (RL-2022-041).

ACKNOWLEDGMENT

This work was supported by the PMCS2I - supercomputer Newton from Ecole Centrale de Lyon, France, member of the FLMSN. The authors thank Matteo Camier and Mickaël Escudero for support on PMCS2I resources.

REFERENCES

(1) Loftsson, T.; Hreinsdóttir, D.; Másson, M. Evaluation of Cyclodextrin Solubilization of Drugs. *Int. J. Pharm.* **2005**, *302*, 18–28. Doi:10.1016/j.ijpharm.2005.05.042.

(2) Alsbaiee, A.; Smith, B. J.; Xiao, L.;Ling, Y.; Helbling, D. E.; Dichtel. W. R. Rapid removal of organic micropollutants from water by a porous b-cyclodextrin polymer. *Nature* **2016**, 529:190-4. Doi:10.1038/nature16185.

(3) Rekharsky, M. V.; Inoue, Y. Complexation Thermodynamics of Cyclodextrins. *Chem. Rev.* **1998**, *98*, 1875–1918. Doi:10.1021/cr970015o.

(4) Škvára, J.; Nezbeda, I.; Izák, P. Molecular Dynamics Study of Racemic Mixtures. Temperature Dependence of the Separation of Ibuprofen Racemic Mixture with *β*-Cyclodextrin in Methanol Solvent. *J. Mol. Liq.* **2020**, *302*, 112575. DOI:10.1016/j.molliq.2020.112575.

(5) González-Méndez, I.; Aguayo-Ortiz, R.; Sorroza-Martínez, K.; Solano, J. D.; Porcu, P.; Rivera, E.; Dominguez, L. Conformational Analysis by NMR and Molecular Dynamics of Adamantane-Doxorubicin Prodrugs and Their Assemblies with β-Cyclodextrin: A Focus on the Design of Platforms for Controlled Drug Delivery. *Bioorg. Med. Chem.* **2020**, *28*, 115510. DOI:10.1016/j.bmc.2020.115510.

(6) Zhao, Q.; Gao, H.; Su, Y.; Huang, T.; Lu, J.; Yu, H.; Ouyang, D. Experimental Characterization and Molecular Dynamic Simulation of Ketoprofen-Cyclodextrin Complexes. *Chem. Phys. Lett.* **2019**, *736*, 136802. DOI:10.1016/j.cplett.2019.136802.

(7) Lipkowitz, K. B. Applications of Computational Chemistry to the Study of Cyclodextrins. *Chem. Rev.* **1998**, *98*, 1829–1874. DOI:10.1021/cr9700179.

(8) Zhao, Q.; Ye, Z.; Su, Y.; Ouyang, D. Predicting Complexation Performance between Cyclodextrins and Guest Molecules by Integrated Machine Learning and Molecular Modeling Techniques. *Acta Pharm. Sin. B* **2019**, *9*, 1241–1252. DOI:10.1016/j.apsb.2019.04.004.

(9) Suárez, D.; Díaz, N. Affinity Calculations of Cyclodextrin Host–Guest Complexes: Assessment of Strengths and Weaknesses of End-Point Free Energy Methods. *J. Chem. Inf. Model.* **2019**, *59*, 421–440. DOI:10.1021/acs.jcim.8b00805.

(10) Linden, L.; Goss, K.-U.; Endo, S. 3D-QSAR Predictions for α-Cyclodextrin Binding Constants Using Quantum Mechanically Based Descriptors. *Chemosphere* **2017**, *169*, 693–699. DOI:10.1016/j.chemosphere.2016.11.115.

(11) Katritzky, A. R.; Fara, D. C.; Yang, H.; Karelson, M.; Suzuki, T.; Solov'ev, V. P.; Varnek, A. Quantitative Structure−Property Relationship Modeling of *β* -Cyclodextrin Complexation Free Energies. *J. Chem. Inf. Comput. Sci.* **2004**, *44*, 529–541. DOI:10.1021/ci034190j.

(12) Benesi, H. A.; Hildebrand, J. H. A Spectrophotometric Investigation of the Interaction of Iodine with Aromatic Hydrocarbons. *J. Am. Chem. Soc.* **1949**, *71*, 2703–2707. DOI:10.1021/ja01176a030.

(13) Higuchi, T.; Connors, K. A. Phase Solubility Techniques. *Advanced Analytical Chemistry of Instrumentation* **1965**, 4, 117-212.

(14) Moreno-Cerezo, J. M.; Córdoba-Díaz, M.; Córdoba-Díaz, D.; Córdoba-Borrego, M. A Stability Study of Tetracycline and Tetracycline Cyclodextrins in Tablets Using a New HPLC Method. *J. Pharm. Biomed. Anal.* **2001**, *26*, 417–426. DOI:10.1016/S0731-7085(01)00416-2.

(15) Li, N.; Zhang, Y.-H.; Wu, Y.-N.; Xiong, X.-L.; Zhang, Y.-H. Inclusion Complex of Trimethoprim with β-Cyclodextrin. *J. Pharm. Biomed. Anal.* **2005**, *39*, 824–829. DOI:10.1016/j.jpba.2005.05.011.

(16) Xu, C.; He, N.; Li, Z.; Chu, Y.; Ding, C.-F. Exploring Halide Anion Affinities to Native Cyclodextrins by Mass Spectrometry and Molecular Modelling. *Eur. J. Mass Spectrom.* **2018**, *24*, 269–278. DOI:10.1177/1469066717748658.

(17) Caira, M. R.; de Vries, E. J. C.; Nassimbeni, L. R. Cyclodextrin Inclusion of P-Hydroxybenzoic Acid Esters. *J. Therm. Anal. Calorim.* **2003**, *73*, 647–651. DOI:10.1023/A:1025446617121.

(18) da Silva, A. J.; dos Santos, E. S. Energetic and Thermodynamical Aspects of the Cyclodextrins-Cannabidiol Complex in Aqueous Solution: A Molecular-Dynamics Study. *Eur. Biophys. J.* **2020**, *49*, 571–589. DOI:10.1007/s00249-020-01463-8.

(19) Li, H.; Chang, S.-L.; Chang, T.-R.; You, Y.; Wang, X.-D.; Wang, L.-W.; Yuan, X.-F.; Tan, M.-H.; Wang, P.-D.; Xu, P.-W.; Gao, W.-B.; Zhao, Q.-S.; Zhao, B. Inclusion Complexes of Cannabidiol with β-Cyclodextrin and Its Derivative: Physicochemical Properties, Water Solubility, and Antioxidant Activity. *J. Mol. Liq.* **2021**, *334*, 116070. DOI:10.1016/j.molliq.2021.116070.

(20) Pan, W.; Zhang, D.; Zhan, J. Theoretical Investigation on the Inclusion of TCDD with β-Cyclodextrin by Performing QM Calculations and MD Simulations. *J. Hazard. Mater.* **2011**, *192*, 1780–1786. DOI:10.1016/j.jhazmat.2011.07.010.

(21) Yan, C.; Liu, C.; Abroshan, H.; Li, Z.; Qiu, R.; Li, G. Surface Modification of Adamantane-Terminated Gold Nanoclusters Using Cyclodextrins. *Phys. Chem. Chem. Phys.* **2016**, *18*, 23358–23364. DOI:10.1039/C6CP04569C.

(22) Tomeček, J.; Čablová, A.; Hromádková, A.; Novotný, J.; Marek, R.; Durník, I.; Kulhánek, P.; Prucková, Z.; Rouchal, M.; Dastychová, L.; Vícha, R. Modes of Micromolar Host-Guest Binding of β-Cyclodextrin Complexes Revealed by NMR Spectroscopy in Salt Water. *J. Org. Chem.* **2021**, *86*, 4483–4496. DOI:10.1021/acs.joc.0c02917.

(23) Caballero, J.; Zamora, C.; Aguayo, D.; Yañez, C.; González-Nilo, F. D. Study of the Interaction between Progesterone and β-Cyclodextrin by Electrochemical Techniques and Steered Molecular Dynamics. *J. Phys. Chem. B* **2008**, *112*, 10194–10201. DOI:10.1021/jp8006766.

(24) Hanpaibool, C.; Chakcharoensap, T.; Arifin; Hijikata, Y.; Irle, S.; Wolschann, P.; Kungwan, N.; Pongsawasdi, P.; Ounjai, P.; Rungrotmongkol, T. Theoretical Analysis of Orientations and Tautomerization of Genistein in *β*-Cyclodextrin. *J. Mol. Liq.* **2018**, *265*, 16–23. DOI:10.1016/j.molliq.2018.05.109.

(25) You, W.; Tang, Z.; Chang, C. A. Potential Mean Force from Umbrella Sampling Simulations: What Can We Learn and What Is Missed? *J. Chem. Theory Comput.* **2019**, *15*, 2433–2443. DOI:10.1021/acs.jctc.8b01142.

(26) Crupi, V.; Ficarra, R.; Guardo, M.; Majolino, D.; Stancanelli, R.; Venuti, V. UV–Vis and FTIR–ATR Spectroscopic Techniques to Study the Inclusion Complexes of Genistein with β-Cyclodextrins. *J. Pharm. Biomed. Anal.* **2007**, *44*, 110–117. DOI:10.1016/j.jpba.2007.01.054.

(27) Chen, M.; Li, Y.-H.; Li, Y.-G.; Li, X.-L.; Zhao, S.-Y.; Yang, L.-J.; Liu, X.-Y.; Zhang, J.-Q. Molecular Dynamics Simulations and Theoretical Calculations of Cyclodextrin-Polydatin Inclusion Complexes. *J. Mol. Struct.* **2021**, *1230*, 129840. DOI:10.1016/j.molstruc.2020.129840.

(28) Rubin, B. S. Bisphenol A: An Endocrine Disruptor with Widespread Exposure and Multiple Effects. *J. Steroid Biochem. Mol. Biol.* **2011**, *127*, 27–34. DOI:10.1016/j.jsbmb.2011.05.002.

(29) Kraemer, S. A.; Ramachandran, A.; Perron, G. G. Antibiotic Pollution in the Environment: From Microbial Ecology to Public Policy. *Microorganisms* **2019**, *7*, 180. DOI:10.3390/microorganisms7060180.

(30) Li, S.; He, B.; Wang, J.; Liu, J.; Hu, X. Risks of Caffeine Residues in the Environment: Necessity for a Targeted Ecopharmacovigilance Program. *Chemosphere* **2020**, *243*, 125343. DOI:10.1016/j.chemosphere.2019.125343.

(31) Yi, M.; Sheng, Q.; Sui, Q.; Lu, H. β-Blockers in the Environment: Distribution, Transformation, and Ecotoxicity. *Environ. Pollut.* **2020**, *266*, 115269. DOI:10.1016/j.envpol.2020.115269.

(32) Kim, S.; Chen, J.; Cheng, T.; Gindulyte, A.; He, J.; He, S.; Li, Q.; Shoemaker, B. A.; Thiessen, P. A.; Yu, B.; Zaslavsky, L.; Zhang, J.; Bolton, E. E. PubChem 2025 Update. *Nucleic Acids Res.* **2025**, *53*, D1516–D1525. DOI:10.1093/nar/gkae1059.

(33) Lecot, S.; Lavigne, A.; Yang, Z.; Géhin, T.; Botella, C.; Jousseaume, V.; Chevolot, Y.; Phaner-Goutorbe, M.; Yeromonahos, C. Arrangement of monofunctional silane molecules on silica surfaces: influence of alkyl chain length, head-group charge, and surface coverage, from molecular dynamics

simulations, X-ray photoelectron spectroscopy, and fourier transform infrared spectroscopy. *J. Phys. Chem. C.* **2020**, 124, 20125 – 20134, DOI: 10.1021/acs.jpcc.0c05349.

(34) Lecot, S.; Lavigne, A.; Yang, Z.; Chevolot, Y.; Phaner-Goutorbe, M.; Yeromonahos, C. Effects of the chemical and structural properties of silane monolayers on the organization of water molecules and ions at interfaces, from molecular dynamics simulations. *Langmuir*, **2021**, 37, 5563 – 5572, DOI:10.1021/acs.langmuir.1c00338.

(35) Lecot, S.; Chevolot, Y.; Phaner-Goutorbe, M.; Yeromonahos, C. Curious Binding Energy Increase between the Receptor-Binding Domain of the SARS-CoV-2 Spike Protein and Angiotensin-Converting Enzyme 2 Adsorbed on a Silane Monolayer from Molecular Dynamics Simulations. *J. Phys. Chem. B* **2021**, *125*, 11078-11090, Doi:10.1021/acs.jpcb.1c06050.

(36) Lecot, S.; Chevolot, Y.; Phaner-Goutorbe, M.; Yeromonahos, C. Impact of Silane Monolayers on the Adsorption of Streptavidin on Silica and its Subsequent Interactions with Biotin: Molecular Dynamics and Steered Molecular Dynamics Simulations. *J. Phys. Chem. B* **2020,** *124*, 6786-6796, Doi:10.1021/acs.jpcb.0c04382.

(37) Chen, J.; Wang, J.; Zhu, W. Zinc ion-induced conformational changes in new Delphi metallo-β-lactamase 1 probed by molecular dynamics simulations and umbrella sampling. *Phys. Chem. Chem. Phys.* **2017**, 19, 3067-3075, DOI:10.1039/C6CP08105C.

(38) Chen, J.; Wang, J.; Zhu, W. Mutation L1196M-induced conformational changes and the drug resistant mechanism of anaplastic lymphoma kinase studied by free energy perturbation and umbrella sampling. *Phys. Chem. Chem. Phys.* **2017**,19, 30239-30248, DOI :10.1039/C7CP05418A.

(39) Lavigne, A.; Géhin, T.; Gilquin, B.; Xerri, L.E.; Veillerot, M.; Jousseaume, V.; Chevolot, Y.; Phaner-Goutorbe, M.; Yeromonahos, C. Effects of the physico-chemical properties of amino acids and chemically functionalized surfaces on DIOS-MS analysis. *Anal. Biochem.* **2025**, 700, 115792, DOI:10.1016/j.ab.2025.115792.

(40) Moreno-Cerezo, J. M.; Córdoba-Díaz, M.; Córdoba-Díaz, D.; Córdoba-Borrego, M. A stability study of tetracycline and tetracycline cyclodextrins in tablets using a new HPLC method, Journal of Pharmaceutical and Biomedical Analysis. *J. Pharm. Biomed.* Anal. **2001,** 26, 417-26, DOI: 10.1016/s0731-7085(01)00416-2.

(41) Li, N.; Zhang, Y. H.; Xiong, X. L.; Li, Z. G.; Jin, X. H.; Wu, Y. N. Study of the physicochemical properties of trimethoprim with β-cyclodextrin in solution. *J. Pharm. Biomed.* Anal. **2005**, 38, 370–374, DOI:10.1016/ j.jpba.2005.01.014.

(42) Wei, Y. L.; Ding, L. H.; Dong, C.; Niu W. P.; Shuang, S. M. Study on inclusion complex of cyclodextrin with methyl xanthine derivatives by fluorimetry. *Spectroc. Acta A* **2003**, 59, 2697–2703, DOI: 10.1016/S1386-1425(03)00058-1.

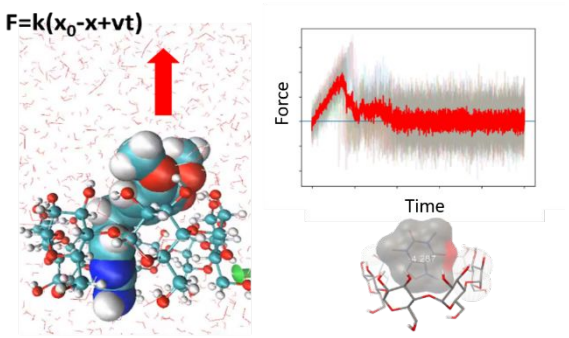
(43) Terekhova, I. V. Interactions of xanthine and its derivatives with cyclodextrins in aqueous solutions. *Russ. Chem. Bull.* **2010**, 59, 533–538, DOI: 10.1007/s11172-010-0142-z.

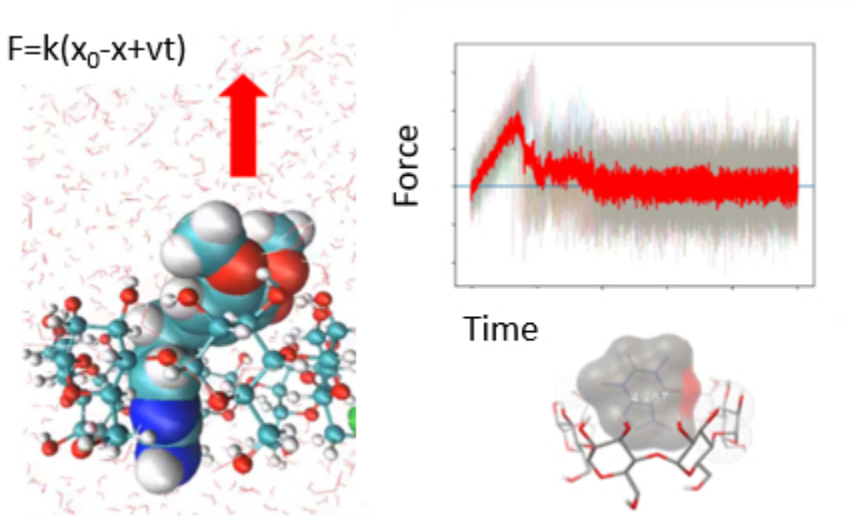
(44) Ficarra, R.; Ficarra, P.; Di Bella, M. R.; Raneri, D.; Tommasini, S.; Calabrò, M. L.; Villari, A.; Coppolino, S. Study of the inclusion complex of atenolol with β-cyclodextrins. *J. Pharm. Biomed.* Anal. **2000**, 23, 231–236, DOI: 10.1016/S0731-7085(00)00274-0.

(45) Vidal, R. B. P.; Ibañez, G. A.; Escandar, G. M. Spectrofluorimetric study of phenolic endocrine disruptors in cyclodextrin. *media RSC Adv.* **2015**, 5, 20914–20923, DOI:10.1039/C4RA13023E.

(46) Barzegar, A.; Moosavi-Movahedi, A.A.; Mahnam, K.; Ashtiani, S.H. Chaperone-like activity of alpha-cyclodextrin via hydrophobic nanocavity to protect native structure of ADH. *Carbohydr Res.* **2010**, 26, 243-9, DOI: 10.1016/j.carres.2009.11.008.

GRAPHIC OF MANUSCRIPT


F=k(x0-x+vt)
Force
Time



Rupture force between organic molecule and β-cyclodextrin calculated by steered molecular dynamics simulations.

75x44mm (150 x 150 DPI)



https://dspace.org/

The complex formation mechanism between -cyclodextrin and organic micropollutants in water, studied by molecular dynamics simulations

De Vince, Oscar; Duan, Zhewen; Yang, Zhugen; Chevolot, Yann; Yeromonahos, Christelle

2026-12-31
American Chemical Society (ACS)
https://doi.org/10.1021/acs.langmuir.5c06371
De Vince O, Duan Z, Yang Z, et al., (2026) The complex formation mechanism between -cyclodextrin and organic micropollutants in water, studied by molecular dynamics simulations. Langmuir, Available online 3 March 2026

Downloaded from a DSpace repository. https://dspace.org/